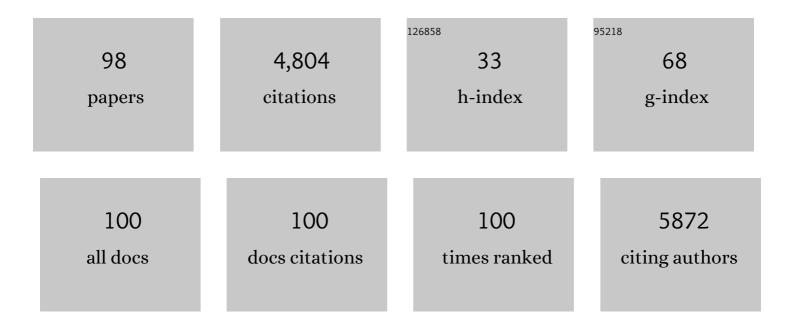
Gregory M Palmer

List of Publications by Year in descending order

Source: https://exaly.com/author-pdf/8596377/publications.pdf Version: 2024-02-01



#	Article	IF	CITATIONS
1	A Spectroscopic Technique to Simultaneously Characterize Fatty Acid Uptake, Mitochondrial Activity, Vascularity, and Oxygen Saturation for Longitudinal Studies In Vivo. Metabolites, 2022, 12, 369.	1.3	3
2	Imaging Hypoxia. , 2021, , 869-895.		0
3	Plasmonic gold nanostars for synergistic photoimmunotherapy to treat cancer. Nanophotonics, 2021, 10, 3295-3302.	2.9	8
4	Cherenkov emissions for studying tumor changes during radiation therapy: An exploratory study in domesticated dogs with naturally-occurring cancer. PLoS ONE, 2020, 15, e0238106.	1.1	2
5	Dual-emissive, oxygen-sensing boron nanoparticles quantify oxygen consumption rate in breast cancer cells. Journal of Biomedical Optics, 2020, 25, .	1.4	6
6	Clinical and Pre-clinical Methods for Quantifying Tumor Hypoxia. Advances in Experimental Medicine and Biology, 2019, 1136, 19-41.	0.8	26
7	Simultaneous in vivo optical quantification of key metabolic and vascular endpoints reveals tumor metabolic diversity in murine breast tumor models. Journal of Biophotonics, 2019, 12, e201800372.	1.1	8
8	Targeting Fluorescent Nanodiamonds to Vascular Endothelial Growth Factor Receptors in Tumor. Bioconjugate Chemistry, 2019, 30, 604-613.	1.8	30
9	Surface-enhanced Raman scattering nanosensors for in vivo detection of nucleic acid targets in a large animal model. Nano Research, 2018, 11, 4005-4016.	5.8	34
10	XIAP Regulation by MNK Links MAPK and NFκB Signaling to Determine an Aggressive Breast Cancer Phenotype. Cancer Research, 2018, 78, 1726-1738.	0.4	45
11	Noninvasive optical spectroscopy for identification of nonâ€melanoma skin cancer: Pilot study. Lasers in Surgery and Medicine, 2018, 50, 246-252.	1.1	9
12	Red blood cell phenotype fidelity following glycerol cryopreservation optimized for research purposes. PLoS ONE, 2018, 13, e0209201.	1.1	25
13	Near-simultaneous quantification of glucose uptake, mitochondrial membrane potential, and vascular parameters in murine flank tumors using quantitative diffuse reflectance and fluorescence spectroscopy. Biomedical Optics Express, 2018, 9, 3399.	1.5	12
14	Development and Preliminary Evaluation of a Murine Model of Chronic Radiation-Induced Proctitis. International Journal of Radiation Oncology Biology Physics, 2018, 101, 1194-1201.	0.4	8
15	Synergistic immuno photothermal nanotherapy (SYMPHONY) to treat unresectable and metastatic cancers and produce and cancer vaccine effect. , 2018, , .		0
16	Assessing effects of pressure on tumor and normal tissue physiology using an automated self-calibrated, pressure-sensing probe for diffuse reflectance spectroscopy. Journal of Biomedical Optics, 2018, 23, 1.	1.4	3
17	Abstract 4152: Synergistic gold nanostar-mediated photothermal and immunotherapy for cancer metastasis treatment. , 2018, , .		0
18	Luminescent Difluoroboron β-Diketonate PLA–PEG Nanoparticle. Biomacromolecules, 2017, 18, 551-561.	2.6	30

#	Article	IF	CITATIONS
19	Miniature spectral imaging device for wide-field quantitative functional imaging of the morphological landscape of breast tumor margins. Journal of Biomedical Optics, 2017, 22, 026007.	1.4	10
20	NIR-emissive PEG-b-TCL micelles for breast tumor imaging and minimally invasive pharmacokinetic analysis. Nanoscale, 2017, 9, 13465-13476.	2.8	17
21	Synergistic Immuno Photothermal Nanotherapy (SYMPHONY) for the Treatment of Unresectable and Metastatic Cancers. Scientific Reports, 2017, 7, 8606.	1.6	113
22	MP98-09 SYNERGISTIC IMMUNO-PHOTOTHERMAL NANOTHERAPY (SYMPHONY): A NOVEL TREATMENT FOR LOCALIZED AND METASTATIC BLADDER CANCER. Journal of Urology, 2017, 197, .	0.2	2
23	Noninvasive measurement of tissue blood oxygenation with Cerenkov imaging during therapeutic radiation delivery. Optics Letters, 2017, 42, 3101.	1.7	9
24	The Development of an In Vivo Mobile Dynamic Microscopy System that Images Cancerous Tumors via Fluorescent and Phosphorescent Nanoparticles. , 2017, , .		0
25	Portable System for Wide-field, Sub-millimeter Functional Imaging of the Morphological Landscape of Breast Tumor Margins. , 2016, , .		0
26	Tunable and amplified Raman gold nanoprobes for effective tracking (TARGET): in vivo sensing and imaging. Nanoscale, 2016, 8, 8486-8494.	2.8	29
27	MEK1/2 inhibitors reverse acute vascular occlusion in mouse models of sickle cell disease. FASEB Journal, 2016, 30, 1171-1186.	0.2	14
28	Renitrosylation of banked human red blood cells improves deformability and reduces adhesivity. Transfusion, 2015, 55, 2452-2463.	0.8	19
29	Effects of High-Dose Microbeam Irradiation on Tumor Microvascular Function and Angiogenesis. Radiation Research, 2015, 183, 147.	0.7	19
30	Modulation of Murine Breast Tumor Vascularity, Hypoxia, and Chemotherapeutic Response by Exercise. Journal of the National Cancer Institute, 2015, 107, .	3.0	188
31	Oxygen Sensing Difluoroboron Dinaphthoylmethane Polylactide. Macromolecules, 2015, 48, 2967-2977.	2.2	117
32	Luminescent Difluoroboron βâ€Điketonate PEGâ€PLA Oxygen Nanosensors for Tumor Imaging. Macromolecular Rapid Communications, 2015, 36, 694-699.	2.0	32
33	Snap-shot multispectral imaging of vascular dynamics in a mouse window-chamber model. Optics Letters, 2015, 40, 3292.	1.7	69
34	Novel Manganese-Porphyrin Superoxide Dismutase-Mimetic Widens the Therapeutic Margin in a Preclinical Head and Neck Cancer Model. International Journal of Radiation Oncology Biology Physics, 2015, 93, 892-900.	0.4	61
35	Biomimetic engineered muscle with capacity for vascular integration and functional maturation in vivo. Proceedings of the National Academy of Sciences of the United States of America, 2014, 111, 5508-5513.	3.3	206
36	Measuring tumor cycling hypoxia and angiogenesis using a sideâ€firing fiber optic probe. Journal of Biophotonics, 2014, 7, 552-564.	1.1	16

#	Article	IF	CITATIONS
37	Systemic anti-tumour effects of local thermally sensitive liposome therapy. International Journal of Hyperthermia, 2014, 30, 385-392.	1.1	22
38	Plasmonics-enhanced and optically modulated delivery of gold nanostars into brain tumor. Nanoscale, 2014, 6, 4078-4082.	2.8	54
39	Hypoxia in Melanoma: Using Optical Spectroscopy and EF5 to Assess Tumor Oxygenation Before and During Regional Chemotherapy for Melanoma. Annals of Surgical Oncology, 2014, 21, 1435-1440.	0.7	8
40	Cellular Migration and Invasion Uncoupled: Increased Migration Is Not an Inexorable Consequence of Epithelial-to-Mesenchymal Transition. Molecular and Cellular Biology, 2014, 34, 3486-3499.	1.1	80
41	Anti-Hypotensive Treatment and Endothelin Blockade Synergistically Antagonize Exercise Fatigue in Rats under Simulated High Altitude. PLoS ONE, 2014, 9, e99309.	1.1	8
42	Imaging the Hypoxic Tumor Microenvironment in Preclinical Models. Cancer Drug Discovery and Development, 2014, , 157-178.	0.2	0
43	Automated Measurement of Microcirculatory Blood Flow Velocity in Pulmonary Metastases of Rats. Journal of Visualized Experiments, 2014, , e51630.	0.2	2
44	Quantitative Mapping of Hemodynamics in the Lung, Brain, and Dorsal Window Chamberâ€Grown Tumors Using a Novel, Automated Algorithm. Microcirculation, 2013, 20, 724-735.	1.0	21
45	Automated measurement of blood flow velocity and direction and hemoglobin oxygen saturation in the rat lung using intravital microscopy. American Journal of Physiology - Lung Cellular and Molecular Physiology, 2013, 304, L86-L91.	1.3	19
46	¹⁸ F-EF5 PET Imaging as an Early Response Biomarker for the Hypoxia-Activated Prodrug SN30000 Combined with Radiation Treatment in a Non–Small Cell Lung Cancer Xenograft Model. Journal of Nuclear Medicine, 2013, 54, 1339-1346.	2.8	31
47	Monitoring of cycling hypoxia and angiogenesis in FaDu head and neck tumors using a side-firing sensor. , 2013, , .		0
48	Sickle Erythrocytes Target Cytotoxics to Hypoxic Tumor Microvessels and Potentiate a Tumoricidal Response. PLoS ONE, 2013, 8, e52543.	1.1	18
49	Wavelength Optimization for Quantitative Spectral Imaging of Breast Tumor Margins. PLoS ONE, 2013, 8, e61767.	1.1	10
50	Abstract B151: Monitoring tumor microenvironment (Hb saturation and oxygenation) in response to plasmonics-assisted photothermal cancer therapy , 2013, , .		0
51	Experimental validation of an inverse fluorescence Monte Carlo model to extract concentrations of metabolically relevant fluorophores from turbid phantoms and a murine tumor model. Journal of Biomedical Optics, 2012, 17, 078003.	1.4	2
52	The combination of theophylline and endothelin receptor antagonism improves exercise performance of rats under simulated high altitude. Journal of Applied Physiology, 2012, 113, 1243-1252.	1.2	10
53	A diffuse reflectance spectral imaging system for tumor margin assessment using custom annular photodiode arrays. Biomedical Optics Express, 2012, 3, 3211.	1.5	20
54	Experimental validation of an inverse fluorescence Monte Carlo model to extract concentrations of metabolically relevant fluorophores from turbid phantoms and a murine tumor model. Journal of Biomedical Optics, 2012, 17, 0780031.	1.4	13

#	Article	IF	CITATIONS
55	Publisher's Note: Experimental validation of an inverse fluorescence Monte Carlo model to extract concentrations of metabolically relevant fluorophores from turbid phantoms and a murine tumor model. Journal of Biomedical Optics, 2012, 17, 0798051.	1.4	1
56	Application of Optical Imaging and Spectroscopy to Radiation Biology. Radiation Research, 2012, 177, 365-375.	0.7	8
57	High-Resolution In Vivo Imaging of Fluorescent Proteins Using Window Chamber Models. Methods in Molecular Biology, 2012, 872, 31-50.	0.4	13
58	A novel angiopoietinâ€derived peptide displays antiâ€angiogenic activity and inhibits tumourâ€induced and retinal neovascularization. British Journal of Pharmacology, 2012, 165, 1891-1903.	2.7	13
59	TH-A-BRB-04: Vascular Response to Microbeam Radiation Therapy in Vivo Using a Murine Window Chamber Tumor Model. Medical Physics, 2012, 39, 3983-3983.	1.6	2
60	In vivo optical molecular imaging and analysis in mice using dorsal window chamber models applied to hypoxia, vasculature and fluorescent reporters. Nature Protocols, 2011, 6, 1355-1366.	5.5	224
61	Molecular Imaging of Hypoxia. Journal of Nuclear Medicine, 2011, 52, 165-168.	2.8	100
62	Non-invasive monitoring of intra-tumor drug concentration and therapeutic response using optical spectroscopy. Journal of Controlled Release, 2010, 142, 457-464.	4.8	86
63	Optical imaging of tumor hypoxia dynamics. Journal of Biomedical Optics, 2010, 15, 1.	1.4	68
64	Utility of functional imaging in prediction or assessment of treatment response and prognosis following thermotherapy. International Journal of Hyperthermia, 2010, 26, 283-293.	1.1	10
65	A low-cost, portable, and quantitative spectral imaging system for application to biological tissues. Optics Express, 2010, 18, 12630.	1.7	22
66	Stereocomplexed Poly(lactic acid)â^'Poly(ethylene glycol) Nanoparticles with Dual-Emissive Boron Dyes for Tumor Accumulation. ACS Nano, 2010, 4, 4989-4996.	7.3	72
67	In Vivo Fluorescence Imaging and Spectroscopy. , 2010, , 30-1-30-11.		1
68	Quantitative Optical Spectroscopy: A Robust Tool for Direct Measurement of Breast Cancer Vascular Oxygenation and Total Hemoglobin Content <i>In vivo</i> . Cancer Research, 2009, 69, 2919-2926.	0.4	154
69	Quantitative diffuse reflectance and fluorescence spectroscopy: tool to monitor tumor physiology in vivo. Journal of Biomedical Optics, 2009, 14, 024010.	1.4	42
70	A Robust Monte Carlo Model for the Extraction of Biological Absorption and Scattering <i>In Vivo</i> . IEEE Transactions on Biomedical Engineering, 2009, 56, 960-968.	2.5	65
71	A dual-emissive-materials design concept enables tumour hypoxia imaging. Nature Materials, 2009, 8, 747-751.	13.3	941
72	Advances in quantitative UV–visible spectroscopy for clinical and pre-clinical application in cancer. Current Opinion in Biotechnology, 2009, 20, 119-131.	3.3	125

#	Article	IF	CITATIONS
73	A strategy for quantitative spectral imaging of tissue absorption and scattering using light emitting diodes and photodiodes. Optics Express, 2009, 17, 1372.	1.7	33
74	Quantitative Physiology of the Precancerous Cervix In Vivo through Optical Spectroscopy. Neoplasia, 2009, 11, 325-332.	2.3	80
75	Electromagnetic Spectroscopy of Normal Breast Tissue Specimens Obtained From Reduction Surgeries: Comparison of Optical and Microwave Properties. IEEE Transactions on Biomedical Engineering, 2008, 55, 2444-2451.	2.5	21
76	Diagnosis of breast cancer using fluorescence and diffuse reflectance spectroscopy: a Monte-Carlo-model-based approach. Journal of Biomedical Optics, 2008, 13, 034015.	1.4	72
77	Monte-Carlo-based model for the extraction of intrinsic fluorescence from turbid media. Journal of Biomedical Optics, 2008, 13, 024017.	1.4	52
78	Cost-effective diffuse reflectance spectroscopy device for quantifying tissue absorption and scattering in vivo. Journal of Biomedical Optics, 2008, 13, 060505.	1.4	38
79	A Miniature Optical Device for Noninvasive, Fast Characterization of Tumor Pathology. , 2008, , .		0
80	Comparison of a physical model and principal component analysis for the diagnosis of epithelial neoplasias in vivo using diffuse reflectance spectroscopy. Optics Express, 2007, 15, 7863.	1.7	45
81	Monte Carlo-based inverse model for calculating tissue optical properties Part I: Theory and validation on synthetic phantoms: erratum. Applied Optics, 2007, 46, 6847.	2.1	11
82	Use of Genetic Algorithms to Optimize Fiber Optic Probe Design for the Extraction of Tissue Optical Properties. IEEE Transactions on Biomedical Engineering, 2007, 54, 1533-1535.	2.5	7
83	Autofluorescence Spectroscopy of Normal and Malignant Human Breast Cell Lines¶. Photochemistry and Photobiology, 2007, 78, 462-469.	1.3	4
84	Monte Carlo-based inverse model for calculating tissue optical properties Part I: Theory and validation on synthetic phantoms. Applied Optics, 2006, 45, 1062.	2.1	276
85	Monte Carlo-based inverse model for calculating tissue optical properties Part II: Application to breast cancer diagnosis. Applied Optics, 2006, 45, 1072.	2.1	116
86	Diagnosis of breast cancer using diffuse reflectance spectroscopy: Comparison of a Monte Carlo versus partial least squares analysis based feature extraction technique. Lasers in Surgery and Medicine, 2006, 38, 714-724.	1.1	97
87	Effect of optical clearing agents on the in vivo optical properties of squamous epithelial tissue. Lasers in Surgery and Medicine, 2006, 38, 920-927.	1.1	21
88	Use of a multiseparation fiber optic probe for the optical diagnosis of breast cancer. Journal of Biomedical Optics, 2005, 10, 024032.	1.4	52
89	Autofluorescence and diffuse reflectance properties of malignant and benign breast tissues. Annals of Surgical Oncology, 2004, 11, 65-70.	0.7	85
90	Investigation of fiber-optic probe designs for optical spectroscopic diagnosis of epithelial pre-cancers. Lasers in Surgery and Medicine, 2004, 34, 25-38.	1.1	65

#	Article	IF	CITATIONS
91	Monte Carlo based inverse model of diffuse reflectance for determination of UV-VIS optical properties and its application to breast cancer diagnosis. , 2004, , .		0
92	The use of a multi-separation probe for optical diagnosis of breast cancer. , 2004, , .		0
93	Diagnosis of Breast Cancer Using Optical Spectroscopy. Medical Laser Application: International Journal for Laser Treatment and Research, 2003, 18, 233-248.	0.4	14
94	Comparison of multiexcitation fluorescence and diffuse reflectance spectroscopy for the diagnosis of breast cancer (march 2003). IEEE Transactions on Biomedical Engineering, 2003, 50, 1233-1242.	2.5	121
95	Autofluorescence Spectroscopy of Normal and Malignant Human Breast Cell Lines¶. Photochemistry and Photobiology, 2003, 78, 462.	1.3	75
96	[21] Steady-state fluorescence imaging of neoplasia. Methods in Enzymology, 2003, 361, 452-481.	0.4	14
97	Optimal methods for fluorescence and diffuse reflectance measurements of tissue biopsy samples. Lasers in Surgery and Medicine, 2002, 30, 191-200.	1.1	69
98	Quantifying the effects of anesthesia on intracellular oxygen via low-cost portable microscopy using dual-emissive nanoparticles. Biomedical Optics Express, 0, , .	1.5	1